

Theoretical characterization of the temperature-dependent saturation magnetization of magnetic metallic materials

Jin-Long Wu(吴金龙), Pan Dong(董攀), Yi He(贺屹), Yan-Li Ma(马艳丽), Zi-Yuan Li(李梓源), Qin-Yuan Yao(姚沁远), Jun Qiu(邱俊), Jian-Zuo Ma(麻建坐), and Wei-Guo Li(李卫国)

Citation: Chin. Phys. B, 2024, 33 (**7**): 077502. DOI: 10.1088/1674-1056/ad39d1
Journal homepage: http://cpb.iphy.ac.cn; http://iopscience.iop.org/cpb

What follows is a list of articles you may be interested in

Localization effect in single crystal of $RuAs_2$

Zhe-Kai Yi(易哲铠), Qi Liu(刘琪), Shuang-Kui Guang(光双魁), Sheng Xu(徐升), Xiao-Yu Yue(岳小宇), Hui Liang(梁慧), Na Li(李娜), Ying Zhou(周颖), Dan-Dan Wu(吴丹丹), Yan Sun(孙燕), Qiu-Ju Li(李秋菊), Peng Cheng(程鹏), Tian-Long Xia(夏天龙), Xue-Feng Sun(孙学峰), and Yi-Yan Wang(王义炎)

Chin. Phys. B, 2024, 33 (**4**): 047501. DOI: 10.1088/1674-1056/ad23d9

Tuning magneto-dielectric properties of Co_2Z ferrites via Gd doping for high-frequency applications

Jian Wu(武剑), Bing Lu(卢冰), Ying Zhang(张颖), Yixin Chen(陈一鑫), Kai Sun(孙凯), Daming Chen(陈大明), Qiang Li(李强), Yingli Liu(刘颖力), and Jie Li(李颉)

Chin. Phys. B, 2023, 32 (**9**): 097501. DOI: 10.1088/1674-1056/acc3f7

Low-temperature ferromagnetism in tensile-strained $LaCoO_{2.5}$ thin film

Yang-Yang Fan(范洋洋), Jing Wang(王晶), Feng-Xia Hu(胡凤霞), Bao-He Li(李宝河), Ai-Cong Geng(耿爱丛), Zhuo Yin(殷卓), Cheng Zhang(张丞), Hou-Bo Zhou(周厚博), Meng-Qin Wang(王梦琴), Zi-Bing Yu(尉紫冰), and Bao-Gen Shen(沈保根)

Chin. Phys. B, 2023, 32 (**8**): 087504. DOI: 10.1088/1674-1056/acafdc

Incommensurate-commensurate magnetic phase transition in double tungstate $Li_2Co(WO_4)_2$

Xiyu Chen(陈西煜), Ning Ding(丁宁), Meifeng Liu(刘美风), Tao Zou(邹涛), V. Ovidiu Garlea, Jingwen Gong(龚婧雯), Fei Liu(刘飞), Yunlong Xie(谢云龙), Lun Yang(杨伦), Shuhan Zheng(郑书翰), Xiuzhang Wang(王秀章), Shuai Dong(董帅), T. Charlton, and Jun-Ming Liu(刘俊明)

Chin. Phys. B, 2022, 31 (**4**): 047501. DOI: 10.1088/1674-1056/ac3818

Magnetocaloric effect and critical behavior of the Mn-rich itinerant material Mn_3GaC with enhanced ferromagnetic interaction

Pengfei Liu(刘鹏飞), Jie Peng(彭杰), Mianqi Xue(薛面起), Bosen Wang(王铂森)

Chin. Phys. B, 2020, 29 (**4**): 047503. DOI: 10.1088/1674-1056/ab7da1

Theoretical characterization of the temperature-dependent saturation magnetization of magnetic metallic materials

Jin-Long Wu(吴金龙)[1,2], Pan Dong(董攀)[2], Yi He(贺屹)[3], Yan-Li Ma(马艳丽)[2], Zi-Yuan Li(李梓源)[2], Qin-Yuan Yao(姚沁远)[2], Jun Qiu(邱俊)[2], Jian-Zuo Ma(麻建坐)[1,2,4], and Wei-Guo Li(李卫国)[1,2,†]

[1] *State Key Laboratory of Coal Mine Disaster Dynamics and Control, Chongqing University, Chongqing* 400044, *China*
[2] *College of Aerospace Engineering, Chongqing University, Chongqing* 400044, *China*
[3] *College of Intelligent Systems Science and Engineering, Hubei Minzu University, Enshi* 445000, *China*
[4] *College of Mechanical Engineering and Automation, Chongqing Industry Polytechnic Colleg, Chongqing* 401120, *China*

(Received 4 February 2024; revised manuscript received 2 April 2024; accepted manuscript online 3 April 2024)

Based on the force–heat equivalence energy density principle, a theoretical model for magnetic metallic materials is developed, which characterizes the temperature-dependent magnetic anisotropy energy by considering the equivalent relationship between magnetic anisotropy energy and heat energy; then the relationship between the magnetic anisotropy constant and saturation magnetization is considered. Finally, we formulate a temperature-dependent model for saturation magnetization, revealing the inherent relationship between temperature and saturation magnetization. Our model predicts the saturation magnetization for nine different magnetic metallic materials at different temperatures, exhibiting satisfactory agreement with experimental data. Additionally, the experimental data used as reference points are at or near room temperature. Compared to other phenomenological theoretical models, this model is considerably more accessible than the data required at 0 K. The index included in our model is set to a constant value, which is equal to $10/3$ for materials other than Fe, Co, and Ni. For transition metals (Fe, Co, and Ni in this paper), the index is 6 in the range of 0 K to $0.65T_{\rm cr}$ ($T_{\rm cr}$ is the critical temperature), and 3 in the range of $0.65T_{\rm cr}$ to $T_{\rm cr}$, unlike other models where the adjustable parameters vary according to each material. In addition, our model provides a new way to design and evaluate magnetic metallic materials with superior magnetic properties over a wide range of temperatures.

Keywords: magnetic metallic materials, temperature dependent, saturation magnetization, modeling

PACS: 75.20.En, 75.50.Cc **DOI:** 10.1088/1674-1056/ad39d1

1. Introduction

Magnetic metallic materials are essential functional materials in modern society.[1] They are widely used as magnetic storage materials in devices, for instance, hard disks, which serve as representative magnetic storage devices for recording, reading, and processing data.[2–4] In addition, magnetic metallic materials make substantial contributions to diverse domains, including rail transport (electric motors in automobiles[5]), aerospace (permanent magnet machines[6]), medicine (magnetic resonance imaging (MRI) scanners[7]), and beyond.[8–14] Nevertheless, magnetic metallic materials frequently experience temperature variations in these aforementioned applications. This becomes particularly critical when the material reaches its critical temperature, as the magnetic metallic material will then cease to function effectively. Saturation magnetization, denoting the maximum magnetization attainable when magnetic metallic materials undergo magnetization within an applied magnetic field, stands as a critical physical parameter employed to assess material performance.[15] A key point to note is that saturation magnetization is strongly influenced by temperature; it gradually decreases as the temperature increases, and once the critical temperature is reached, the saturation magnetization drops to zero. Therefore, investigation of the temperature dependence of saturation magnetization is vital to comprehend the safety and reliability of magnetic metallic materials in practical applications. It is necessary to establish a quantitative relationship between saturation magnetization and temperature. In addition, our model also furnishes some theoretical basis for the design of magnetic devices.[16]

Experimentally, Kuz'min investigated the temperature dependence of saturation magnetization in Sm_2Fe_{17}, employing a static magnetic field of 14 T.[17] Crangle conducted measurements of the saturation magnetization for Fe and Ni at varying temperatures.[18] Simultaneously, other researchers have undertaken analogous experimental investigations on diverse magnetic metallic materials. These studies consistently demonstrate that the saturation magnetization gradually diminishes as the temperature increases. Upon reaching the critical temperature, saturation magnetization rapidly declines to zero. Thereafter, with further temperature elevation, saturation magnetization exhibits no significant variations.

Theoretical studies have explored the temperature-dependent behavior of saturation magnetization, and several scholars have put forward models to explain this phenomenon. Bloch's law elucidates the reduction in macroscopic magne-

†Corresponding author. E-mail: wgli@cqu.edu.cn

© 2024 Chinese Physical Society and IOP Publishing Ltd

tization stemming from the thermal excitation of spin waves within a magnet:[19]

$$M_{\rm s}(T) = M_{\rm s}(0)\left[1-\left(\frac{T}{T_{\rm c}}\right)^{\alpha}\right], \tag{1}$$

where $M_{\rm s}(0)$ is the saturation magnetization at 0 K. However, experimental data near 0 K are not easy to obtain. Here, $T_{\rm c}$ denotes the Curie temperature, at which the $M_{\rm s}$ becomes zero. The index α represents Bloch's index which, for bulk materials, has a value of $3/2$. Bloch derived the $T^{3/2}$ law by considering the magnon excitation of long-wave-length spin waves at low temperatures. This model is exclusively applicable to magnetic metallic materials at temperatures significantly below the Curie temperature. Consequently, the subsequent model comparisons did not involve a comparison with this particular model.

In the low-temperature limit, $m(T) = M(T)/M(0)$ can be calculated from $m(T) = 1-\rho(T)$, where $\rho(T) = (1/N)\sum_{\boldsymbol{k}} n_{\boldsymbol{k}}$ is the sum over the wave vector $\boldsymbol{k}$ of the spin-wave occupation number in the Brillouin zone.[20] The integral $\rho(T) = (1/N)\sum_{\boldsymbol{k}} n_{\boldsymbol{k}}$ at low temperatures for both quantum and classical statistics is a very well-known result. For the classical statistics,[16]

$$m_{\rm c}(T) \approx 1-\frac{1}{3}\frac{T}{T_{\rm c}}, \tag{2}$$

where $T_{\rm c}$ is the Curie temperature. Under the same conditions, for quantum statistics,[16]

$$m_{\rm q}(T) \approx 1-\frac{1}{3}s\left(\frac{T}{T_{\rm c}}\right)^{3/2}, \tag{3}$$

where s is the slope factor. Classical and quantum expressions $m(T)$ can be mapped by Eq. (2) and Eq. (3)

$$m(\tau) = (1-\tau)^{\beta}. \tag{4}$$

Equation (4) can be employed for calculations when the temperature approaches the Curie temperature, with τ being equivalent to $T/T_{\rm c}$ and β approximately equal to $1/3$. Likewise, Eqs. (2) and (3) are solely relevant at extremely low temperatures, whereas Eq. (4) finds applicability in proximity to the Curie temperature. Consequently, these models are not subjected to comparison with our model in subsequent analyses. Building upon this foundation and in alignment with Bloch's law, the Curie–Bloch model (C-B model) is formulated as follows:[21]

$$m(\tau) = (1-\tau^{q})^{\beta}, \tag{5}$$

where q is an empirical constant. Kuz'min considers that there is no general analytical expression for $m(\tau)$ beyond the molecular field approximation,[22] except in the two limit cases $\tau \to 0$ and $\tau \to 1$. Although it has recently been shown that an accurate description of $m(\tau)$ over the whole interval $0 < \tau < 1$ is provided by a combination of two (in some cases, three) simple power laws: one for each of the temperature subintervals. Kuz'min proposes an alternative form of the Curie–Bloch model:[22]

$$m(\tau) = \left(1-r\tau^{3/2}-(1-r)\tau^{p}\right)^{\eta}, \tag{6}$$

where the parameters r and p can be considered fitting parameters,[16] with $p > 3/2$ and $r > 0$. The η here is the same as the β in Eq. (5), and the Heisenberg critical exponent is $1/3$[23] for ferromagnetic metallic materials. The values of r and p then depend on the form of the temperature-dependent curve of $m(\tau)$. The analysis of Kuz'min was carried out to fit the experimental data obtained, and it was found that the value of the p for most magnetic metallic materials could be taken as $5/2$, except for iron, where the value of the p was taken as 4. When $\tau \to 0$, it takes the same form as in Eq. (3), whereas in the critical region, when $\tau \to 1$, m is proportional to Eq. (4), as prompted by the critical behavior of the Heisenberg model.[23]

Liu[24–26] studied the influence of temperature on saturation magnetization from both macroscopic and microphysical perspectives. They conducted numerical simulations to investigate the microscopic properties of magnetic materials, providing a basis for further research on the factors affecting saturation magnetization. This work laid the foundation for the subsequent development of a temperature-dependent theoretical model of saturation magnetization with a stronger physical background.

Equations (1), (5), and (6) are frequently employed to compute saturation magnetization as a function of temperature. Equation (1) is familiar and used by people, and provides reasonably accurate predictions, primarily within the extreme low-temperature range. And the C-B model and Kuz'min model have good prediction ability for most of the experimental data when the saturation magnetization is around 0 K and the fitting parameters (the C-B model contains one and the Kuz'min model contains two) in their respective models are determined. In addition, in the Kuz'min model, the value of fitting parameter p is not explained in the literature (the p-value for iron is regarded as 4, while for other magnetic metallic materials it is $5/2$). It is also noteworthy that they depend on choosing an experimental value in close proximity to 0 K as a reference point. The acquisition of such experimental data at exceedingly low temperatures is not easy to obtain, rendering these equations less suitable for engineering applications. To address this inconvenience, it is vital to develop a theoretical characterization model for characterizing saturation magnetization at various temperatures that are better suited for engineering applications.

In this paper, a simple and highly effective model is constructed to accurately predict the saturation magnetization in magnetic metallic materials at different temperatures. Our

model demonstrates good agreement with established experimental data and undergoes a comprehensive comparison with the traditional models commonly used in the field. We propose to use experimental data collected at room temperature and its immediate vicinity as reference points, as these can be easily obtained by experimental means. Additionally, our model provides a novel perspective for comprehending the intricate correlation between temperature and saturation magnetization in magnetic metallic materials.

2. Theoretical model

2.1. The explanation of the force–heat equivalence energy density principle

From the perspective of material failure, both the work done by the external stress (strain energy) and the heat absorbed from the outside contribute to the failure of the material. There is also an equivalent relationship between the external stress and the contribution of the heat absorbed from the outside to the failure of the material. It is therefore assumed that there is a fixed maximum energy from when the material is intact to failure. This energy consists of strain energy and heat energy, and there is an equivalence relationship between the two, which can be expressed by an equivalence coefficient.[27]

2.2. The justification of the force–heat equivalence energy density principle

A large number of past works have fully verified the rationality of this hypothesis. Based on the proposed force–heat equivalence energy density principle, we have developed a series of novel theoretical characterization models of materials; for example, temperature-dependent models of yield strength, ultimate tensile strength, and fatigue strength for metallic materials.[28–30] Furthermore, the proposed force–heat equivalence energy density principle has been successfully extended to the theoretical characterization of the physical properties of materials, such as the temperature-dependent anti-phase boundary energy, vacancy formation energy, surface energy, grain boundary slip energy and dislocation climbing energy of the metallic materials,[31–35] and the temperature-dependent band gap, refractive index and Raman frequency of semiconductor materials.[36–38] These models offer a quantitative description of the properties affected by temperature due to the change in heat energy. Additionally, by utilizing the force–heat equivalence energy density principle as an ideological approach, the saturation magnetization of magnetic metallic materials can be expressed quantitatively as a function of temperature.

Magnetic anisotropy energy is defined as the saturation magnetization in the magnetic material that is required to take different directions and change the energy. Specifically, in an applied magnetic field, it is the magnetization energy required along the magnetic material within the different magnetization directions (from the non-magnetic state to the saturation magnetization-state-required energy, also known as the magnetic material in the external magnetic field magnetization process stored energy) is different. Basically, along the same magnetization direction, the magnetic anisotropy energy and magnetization energy are equal in numerical magnitude. Also, because there are relationships between the magnetic anisotropy energy and the magnetic anisotropy constant and the saturation magnetization, the concept of magnetic anisotropy energy rather than magnetization energy is used in Eq. (7). At the same temperature, the magnetization energy required along a magnetization direction does not change; as the temperature increases, the heat energy increases, and the thermal motion of atoms and molecules inside the material becomes more intense, resulting in the direction of the magnetic domains becoming more chaotic, thereby reducing the saturation magnetization of magnetic materials. Therefore, the magnetization energy required to magnetize it to a saturated state will also be reduced.

The previous work of our research group has successfully extended the force–heat equivalence energy density principle to the temperature-dependent physical property characterization of materials. Similarly, based on the equivalence principle of the force–heat equivalence energy density principle and combined with their theoretical method for temperature-dependent physical property characterization, we applied it to the temperature-dependent theoretical characterization of saturated magnetization: for magnetic materials, along a specific magnetization direction, it is assumed that there is a fixed and constant maximum energy value corresponding to the magnetic material under an applied magnetic field from the state with maximum saturation magnetization to the state with no saturation magnetization (corresponding to 0 K to the critical temperature). This fixed maximum energy value is composed of the magnetization energy absorbed from the external magnetic field (numerically equal to the magnetic anisotropy energy) and the external heat energy absorbed, both of which contribute to the saturation magnetization. There is also an equivalence relationship between the two, which can be expressed by an equivalence coefficient. i.e.,

$$W_{\mathrm{Total}} = \lambda W_{\mathrm{T}}(T) + W_{\mathrm{A}}(T), \tag{7}$$

where W_{Total} is the maximum energy; $W_{\mathrm{T}}(T)$ is the increment of the heat energy; λ is the conversion coefficient between the heat energy and the magnetic anisotropy energy; and $W_{\mathrm{A}}(T)$ is the magnetic anisotropy energy at temperature T.

The heat energy $W_{\mathrm{T}}(T)$ at different temperatures can be expressed as the specific heat capacity at constant pressure

$$W_{\mathrm{T}}(T) = \int_0^T \rho_{\mathrm{m}} C_{\mathrm{p}}(T)\,\mathrm{d}T, \tag{8}$$

where ρ_{m} is the density of materials (it shows a weak temperature correlation, so its temperature correlation is ignored), and $C_{\mathrm{p}}(T)$ is the temperature-dependent specific heat capacity at constant pressure.

The temperature dependence of magnetic anisotropy is caused by heat fluctuations in magnetization.[16] Basically, temperature can change the temperature-dependent magnetic anisotropy by affecting the magnetization. Therefore, we extend the expression of the magnetic anisotropy energy at room temperature to arbitrary temperature T, for tetragonal and hexagonal crystals and triangular crystals, which can be expressed by the following equation:[39]

$$W_{\mathrm{A}}(T) = K(T)\sin^2\theta, \tag{9}$$

where $K(T)$ is the magnetic anisotropy constant at temperature T, and θ is the angle between the direction of magnetization and the axis of easy magnetization. The same thing applies to cubic crystals, which can be expressed by the following equation after ignoring the higher-order terms:[40]

$$W_{\mathrm{A}}(T) = K(T)(\alpha_1^2\alpha_2^2 + \alpha_2^2\alpha_3^2 + \alpha_1^2\alpha_3^2), \tag{10}$$

where α_1, α_2 and α_3 are the direction cosines of the magnetization with respect to the crystal axes angle.

If Eqs. (9) and (10) are subjected to a simple mathematical transformation, the following equation can be obtained:

$$W_{\mathrm{A}}(T)/W_{\mathrm{A}}(T_0) = K(T)/K(T_0). \tag{11}$$

The magnetic anisotropy constant is related to the saturation magnetization as follows:[41]

$$K(T)/K(T_0) = [M_{\mathrm{s}}(T)/M_{\mathrm{s}}(T_0)]^n. \tag{12}$$

This model is actually an empirical model, and scholars have found such a power exponential relationship through a large number of experiments. However, it should be noted that Eq. (12) does not apply to all magnetic metal materials; it is only applicable to rare earth metals and their intermetallic compounds and transition metal elemental magnetic materials that do not undergo spin reorientation internally. Basically, it does not apply to those materials where spin reorientation occurs due to strong crystalline anisotropy. For example, the change in the crystalline anisotropy of $Nd_2Fe_{14}B$ is very complicated, and therefore spin reorientation phenomena are observed for this material.[42,43] This will also be an issue to be addressed in our follow-up work. Therefore, the model that is finally established in this paper is also not applicable to materials where internal spin reorientation occurs. Here $M_{\mathrm{s}}(T)$ and $M_{\mathrm{s}}(T_0)$ are the saturation magnetization at temperature T and the reference temperature T_0, and n is a temperature-independent index.

When $T = T_0$, it can be obtained that

$$W_{\mathrm{Total}} = \lambda W_{\mathrm{T}}(T_0) + W_{\mathrm{A}}(T_0). \tag{13}$$

When the temperature reaches the critical temperature, the saturation magnetization value will be zero, as we can see from Eqs. (11) and (12); the corresponding magnetic anisotropy energy will be zero.

When $T = T_{\mathrm{cr}}$, it can be obtained that

$$W_{\mathrm{Total}} = \lambda W_{\mathrm{T}}(T_{\mathrm{cr}}), \tag{14}$$

where T_{cr} is the critical temperature (Curie temperature or Néel temperature).

By combining Eqs. (13) and (14), the following equations are obtained:

$$\lambda = \frac{W_{\mathrm{A}}(T_0)}{W_{\mathrm{T}}(T_{\mathrm{cr}}) - W_{\mathrm{T}}(T_0)}, \tag{15}$$

$$W_{\mathrm{Total}} = \frac{W_{\mathrm{A}}(T_0)}{W_{\mathrm{T}}(T_{\mathrm{cr}}) - W_{\mathrm{T}}(T_0)} W_{\mathrm{T}}(T_{\mathrm{cr}}). \tag{16}$$

Hence, we can derive the following equation by substituting Eqs. (11), (15), and (16) into Eq. (13):

$$W_{\mathrm{A}}(T) = W_{\mathrm{A}}(T_0)\left(1 - \frac{\int_{T_0}^{T} C_{\mathrm{p}}(T)\,\mathrm{d}T}{\int_{T_0}^{T_{\mathrm{cr}}} C_{\mathrm{p}}(T)\,\mathrm{d}T}\right). \tag{17}$$

By combining Eqs. (11) and (12) with Eq. (17), the temperature-dependent saturation magnetization model of the final model can be obtained

$$M_{\mathrm{s}}(T) = M_{\mathrm{s}}(T_0)\left(1 - \frac{\int_{T_0}^{T} C_{\mathrm{p}}(T)\,\mathrm{d}T}{\int_{T_0}^{T_{\mathrm{cr}}} C_{\mathrm{p}}(T)\,\mathrm{d}T}\right)^{1/n}. \tag{18}$$

The temperature-dependent specific heat of the material described in the text can be easily obtained from material handbooks and references. It should be noted that Eq. (18) and the subsequent model (Eqs. (19) and (20)) are only applicable to rare earth metals and their intermetallic compounds and transition metal elemental magnetic materials that do not undergo spin reorientation internally. Basically, it does not apply to those materials where spin reorientation occurs due to strong crystalline anisotropy.

Specifically, in our model, there is one parameter n, whose physical meaning is not very clear; the rest of the parameters have clear physical meaning, and all are easily accessible. In the C-B model, q has no clear physical meaning. In the Kuz'min model, r and p have no clear physical meaning. But there is no denying that the physical value of both models is of great significance.

3. Results

By employing Eq. (18), we predict the saturation magnetization for nine distinct magnetic metallic materials. Subsequently, these predictions are compared with the corresponding experimental values, which are documented in the reference list provided within the source of the experimental data presented in Tables 1 and 2. As previously noted, our model possesses an advantage over their model concerning the selection of reference points. Whereas their model is limited to choosing points near 0 K, our model can select points at or near room temperature. Data points in the vicinity of room temperature are more accessible than those near 0 K. From both a technical application and experimental cost standpoint, opting for data at or near room temperature as the reference point is more reasonable. Consequently, in Figs. 1 and 2, our model employs room temperature as the reference point for calculations. At the same time, Tables 1 and 2 provide the requisite parameters for model computation. The values for parameters T_0, $M_s(T_0)$, and T_{cr} are extracted from the referenced experimental data, and the essential heat capacity data are sourced from the listed reference for heat capacity.

Table 1. Material parameters for magnetic metallic materials.

Material parameters	T_0 (K)	$M_s(T_0)$ (emu/g)	T_{cr} (K)	Experimental data	Heat capacity
Sm_2Fe_{17}	301.25	112.06	380.00	[17]	[44]
Y_2Fe_{17}	298.27	77.18	312.00	[22]	[45]
Fe	292.30	217.60	1044.00	[18]	[46]
Co	291.41	162.76	1385.00	[47]	[46]
Ni	303.54	54.86	631.00	[18]	[46]
	290.12	54.20	628.00	[48]	
Dy	174.36	138.00	179.00	[49]	[50]
Tb	221.08	140.44	232.00	[49]	[51]

Table 2. Material parameters for magnetic metallic materials.

Material parameters	T (K)	$M_s(T_0)$ (μ_B/f.u.)	T_{cr} (K)	Experimental data	Heat capacity
Nd_2Fe_{17}	300.38	24.14	348.00	[52]	[53]

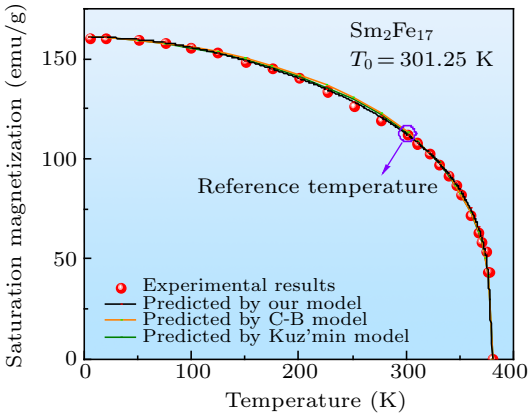


Fig. 1. Comparison of the predicted results from our model and previous models, and experimental data of Sm_2Fe_{17} of the temperature dependence of the saturation magnetization.

Upon analyzing Fig. 1 and combining the C-B model and Kuz'min model, we find that the predicted outcomes for Sm_2Fe_{17} from our model closely align with the experimental results when the index n in Eq. (18) is set to $10/3$. Building upon this observation, we postulate that for other magnetic metallic materials, n can also be approximated as $10/3$. To substantiate this hypothesis, we have generated predictions for six distinct sets of experimental data (Y_2Fe_{17}, Nd_2Fe_{17}, Dy, and Tb) using Eq. (18). These results are depicted in Fig. 2.

As illustrated in Fig. 2, due to the strong agreement between the predicted and experimental results, it is reasonable to conclude that the index n can be set as $10/3$. Consequently, the definitive expression in the temperature-dependent saturation magnetization model for magnetic metallic materials can be formulated as follows:

$$M_s(T) = M_s(T_0)\left(1 - \frac{\int_{T_0}^{T} C_p(T)\,\mathrm{d}T}{\int_{T_0}^{T_{cr}} C_p(T)\,\mathrm{d}T}\right)^{3/10}. \quad (19)$$

Our model (Eq. (19)) establishes a clear correlation between saturation magnetization and temperature. Our model relies solely on the saturation magnetization of magnetic metallic materials at or near room temperature or can predict its saturation magnetization at different temperatures. This is advantageous compared with the other two models, which need to choose the saturation magnetization at 0 K. It should be noted that the reference point selected by our model has been marked in Fig. 2, and the reference point selected by the C-B and Kuz'min models is the first experimental data point. In addition, the n value in our model is a fixed value of $10/3$, while the r and q values in the other two models are different values for different materials.

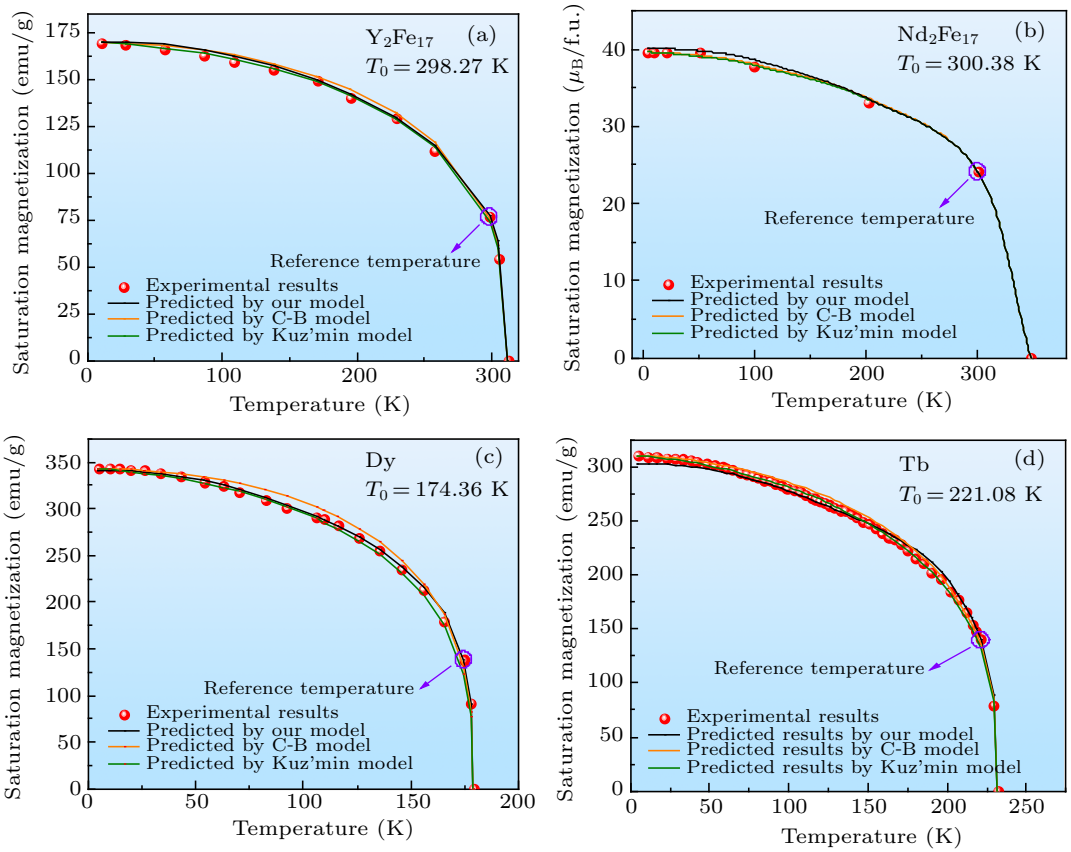


Fig. 2. Comparison of the predicted results from our model and previous models, and experimental data of four sets of the temperature dependence of the saturation magnetization.

4. Discussion

Referring to Figs. 1 and 2, our model consistently exhibits strong agreement with the seven sets of experimental data, as well as with the predictions of other models. Notably, the index n in our model maintains a consistent value of $10/3$ for all the aforementioned materials, in contrast to the q in the C-B model and the r in the Kuz'min model, which are determined through fitting and yield distinct values for each material.

As depicted in Figs. 2(a) and 2(b), the magnetic metallic materials, Y_2Fe_{17} and Nd_2Fe_{17}, belong to the category of Y–Fe–B magnets and Nd–Fe–B magnets; they are widely used in the field of motors. From Figs. 2(a) and 2(b), it can be seen that the prediction results of our model and the other two models are in good agreement with the experimental results. The prediction accuracy of the Kuz'min model is slightly higher, which may contain two fitting parameters, which can better control the fitting accuracy. The fitting accuracy of the C-B model is similar to ours.

Regarding the two antiferromagnetic metallic materials Dy and Tb, as illustrated in Figs. 2(c) and 2(d), their Néel temperatures, defined as the temperatures at which their saturation magnetization reaches zero, are 179 K and 232 K, respectively.[49] This indicates that these materials will display external magnetism below their respective Néel temperatures when exposed to an applied magnetic field. As seen in Figs. 2(c) and 2(d), there are obvious differences between the prediction results of the C-B model and the experimental results, especially for Dy; the predicted results are quite different from the experimental results, but they are within a reasonable margin of error. The prediction results of our model are in good agreement with the experimental results.

In our study, we employed Eq. (19) to calculate the magnetic properties of three 3d pure transition metals: Fe, Ni, and Co. It is worth noting that for Ni, we gathered experimental data from two distinct sources. These materials are recognized for their substantial saturation magnetization at room temperature, making them suitable as magnetic metallic materials for various applications. In addition, the Curie temperatures of Fe and Co greatly exceed room temperature, expanding their potential utility as magnetic functional materials at both room and elevated temperatures. When n is taken as $10/3$, it is found that there is a slightly significant difference between the predicted results and the experimental results (the black line is shown in Fig. 4). The maximum error between the predicted value and the experimental value is within 7%, which is also within a reasonable error range. However, compared to the prediction results of the other two models, the prediction accuracy of Eq. (19) is still quite different and, in some practical applications, the prediction accuracy of the model is required to reach a high level; therefore, $10/3$ is not the best value for Fe, Co and Ni materials. According to the literature,[54] the possible reason for the above phenomenon is that the mag-

netic properties of 3d transition pure metal elements (Fe, Co, and Ni in this paper) are quite different from those of rare earth metals and their intermetallic compounds. There are also differences in the microscopic theories that explain the reasons for the macroscopic magnetism of the two, and the magnetism of the rare earth metals and their intermetallic compounds can be explained by the local electron theory: the theory states that the electrons are confined to a particular atom. Therefore, the magnetism is mainly determined by the spin of the electrons and their interaction between the atoms. These local magnetic moments interact with each other through exchange or other indirect interactions, resulting in the production of macroscopic magnetism. However, the magnetic properties of 3d transition pure metals cannot be explained by the local electron theory, but can be explained by the traveling electron theory: the theory assumes that 3d electrons can move freely in the crystal, and the periodic potential field of the crystal causes the energy of the electrons to change with the wave vector to form a band and a band gap. The interaction between the electrons causes the uneven distribution of the band and band gap in the metal, resulting in macroscopic magnetism. The reasons for the magnetic generation of the two are different, and saturation magnetization, as an important embodiment of its magnetism, will also differ from the law of temperature evolution. Therefore, when n is $10/3$, the theoretical difference in the generation of macroscopic magnetism is one of the reasons why the predicted results of Eq. (19) do not agree well with the experimental results of Fe, Co, and Ni. After researching the literature, it was discovered that for our model, n can be either 10 or 6 within the range of 0 K to approximately $0.65T_{\rm cr}$, and n can be 3 within the range of $0.65T_{\rm cr}$ to $T_{\rm cr}$.[55–57] The reason for setting n as 6 within the range of 0 K to approximately $0.65T_{\rm cr}$ is due to its higher prediction accuracy compared to when setting n as 10. As shown in Fig. 3, the prediction accuracy of our model with $n = 6$ is obviously higher than that with $n = 10$. Therefore, finally, we take n to be 6 from 0 K to $0.65T_{\rm cr}$.

In summary, for materials other than Fe, Co, and Ni in this paper, n is $10/3$ and the predicted results are found to be in good agreement with the experimental results. For materials such as Fe, Co, and Ni, n is 6 in the range from 0 K to $0.65T_{\rm cr}$, and n is 3 in the range from $0.65T_{\rm cr}$ to $T_{\rm cr}$, and the predicted results are found to be in good agreement with the experimental results. Based on the above analysis, Eq. (18) can be rewritten as

$$M_{\rm s}(T)=\begin{cases} M_{\rm s}(T_0)\left(1-\dfrac{\int_{T_0}^{T}C_{\rm p}(T)\,{\rm d}T}{\int_{T_0}^{T_{\rm cr}}C_{\rm p}(T)\,{\rm d}T}\right)^{1/6}, & T\le 0.65T_{\rm cr},\\ M_{\rm s}(T_x)\left(1-\dfrac{\int_{T_x}^{T}C_{\rm p}(T)\,{\rm d}T}{\int_{T_x}^{T_{\rm cr}}C_{\rm p}(T)\,{\rm d}T}\right)^{1/3}, & T_{\rm cr}\ge T>0.65T_{\rm cr}, \end{cases} \tag{20}$$

where T_x is the temperature point less than or equal to $0.65T_{\rm cr}$. As shown in Fig. 4 (the yellow line is shown), the predictions of our model (Eq. (20)) show a remarkable agreement with the experimental results.

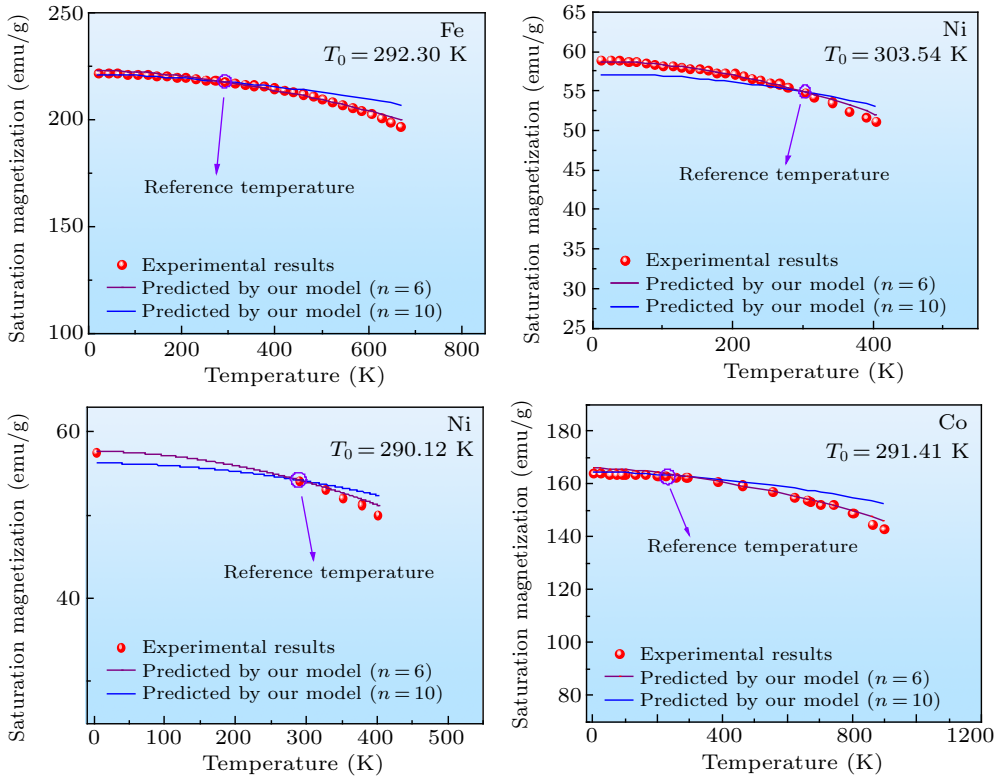


Fig. 3. The predictions of $n = 10$ and $n = 6$ are compared with the experimental results in the range 0 K to $0.65T_{\rm cr}$ for Fe, Ni, and Co.

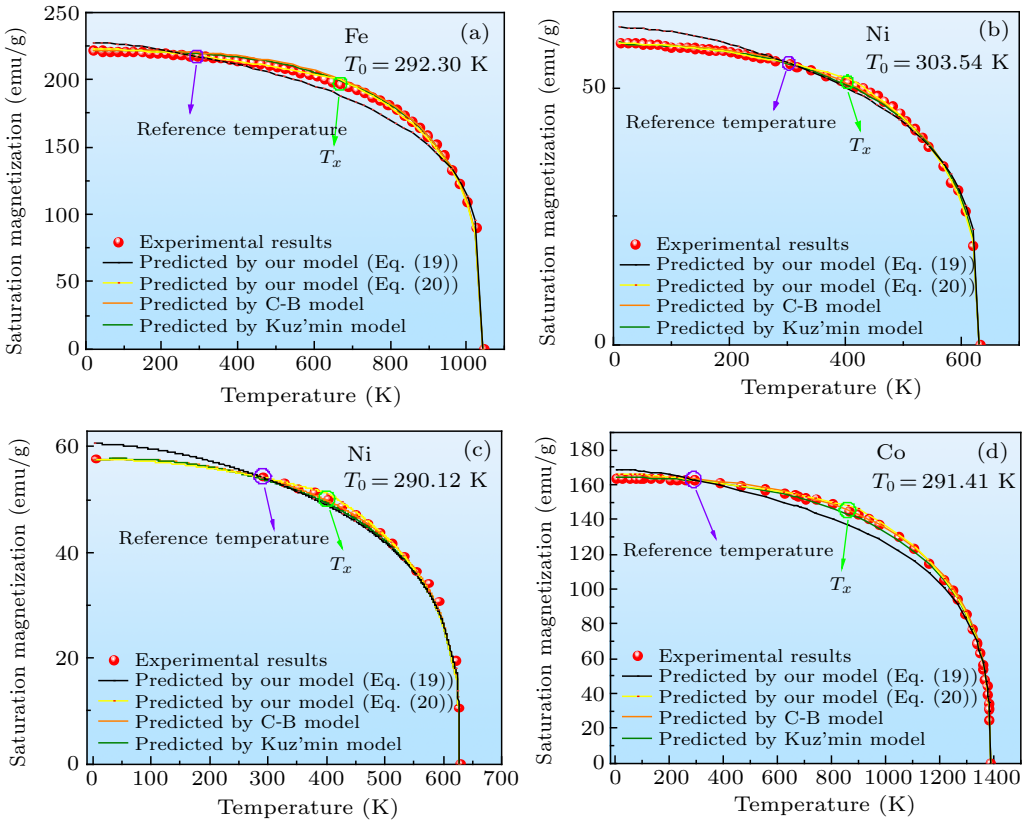


Fig. 4. Comparison of the predicted results from our model and previous models, and experimental data of four sets of the temperature dependence of the saturation magnetization.

For 3d transition pure metals, it is essential to emphasize that the value of q in the C-B model and the value of r in the Kuz'min model (for Fe, the p-value is 4, and for Co and Ni, it is 5/2) vary for each set of experimental data. Our model (Eq. (20)) takes a fixed value (6 and 3) in two temperature segments for 3d transition pure metals. Our model also has other advantages. In practical engineering applications, it is customary to select reference points at or near room temperature as the reference point. However, the C-B and Kuz'min models can only utilize experimental values close to 0 K as reference points, which proves to be inconvenient for engineering applications. The choice of reference points at or near room temperature is well justified by the convenience of obtaining saturation magnetization values at room temperature compared to other temperatures. This is because saturation magnetization values at room temperature are not only easier to obtain than at other temperatures.

In summary, when dealing with magnetic metallic materials that have a critical temperature above room temperature, the reference point for the saturation magnetization value is at room temperature. For materials with a critical temperature below room temperature, such as Dy and Tb, the reference point should be selected as close to room temperature as possible.

5. Conclusion

In summary, this study presents a temperature-dependent theoretical model for characterizing the saturation magnetization of magnetic metallic materials. The model has been validated using experimental data from nine different magnetic metallic materials, and the predictions show good agreement with the experimental results. Our model has an advantage over others as it uses experimental data near room temperature as a reference point, rather than relying solely on data near 0 K. Obtaining experimental data at room temperature is more convenient and requires less effort than collecting data at 0 K. In our model, the index n remains 10/3 for available experimental data, except for Fe, Co, and Ni, where it is 6 in the range of 0 K to $0.65T_{\rm cr}$, and 3 in the range of $0.65T_{\rm cr}$ to $T_{\rm cr}$. This sets our model apart from others, where adjustable parameters vary for each material. The prediction results of our model and the other two models are in good agreement with the experimental results from perspectives. However, there are differences in prediction accuracy for some specific materials. Additionally, our model includes a parameter n, whose physical meaning is unclear. All the other parameters have clear physical meanings. The C-B model does not have a clear physical meaning for q, while the Kuz'min model lacks clear physical meanings for r and p. Despite this, both models have undeniable physical value, and they have advantages over our model in terms of mathematical complexity. In addition, we

present a new approach with theoretical basis for predicting the temperature-dependent saturation magnetization of magnetic metallic materials.

Acknowledgement

Project supported by the Natural Science Foundation of Chongqing (Grant No. CSTB2022NSCQ-MSX0391).

References

[1] Zhang Y, Wang Z and Cao J 2013 *J. Appl. Phys.* **113** 017203
[2] Plumer M L, Van Ek J and Weller D 2001 *The physics of ultra-high-density magnetic recording* (Vol. 41) (Japan: Springer Science & Business Media)
[3] Parkin S S, Hayashi M and Thomas L J S 2008 *Science* **320** 190
[4] Wolf S, Awschalom D, Buhrman R, Daughton J, Von Molnár S and Roukes M 2001 *Science.* **294** 1488
[5] Matsuura Y 2006 *J. Magn. Magn. Mater.* **303** 344
[6] Liu S J 2019 *Chin. Phys. B* **28** 017501
[7] Riley M, Walmsley A and Speight J 2002 *Mater. Sci. Tech.* **18** 112
[8] Gutfleisch O, Willard M A, Brück E, Chen C H, Sankar S and Liu J P 2011 *Adv. Mater.* **23** 821
[9] Fingers R T and Rubertus C S 2000 *IEEE T. Magn.* **36** 3373
[10] Gutfleisch O, Müller K H, Khlopkov K, Wolf M, Yan A, Schäfer R, Gemming T and Schultz L 2006 *Acta Mater.* **54** 997
[11] Provenza A J, Montague G T, Jansen M J and Palazzolo A B 2005 *J. Eng. Gas. Turbines. Power.* **127** 437
[12] Zverev V, Pyatakov A, Shtil A and Tishin A 2018 *J. Magn. Magn. Mater.* **459** 182
[13] Jordan A, Scholz R, Wust P, Fähling H and Felix R 1999 *J. Magn. Magn. Mater.* **201** 413
[14] Kok M, Qadir R A and Mohammed S S 2022 *Eur. Phys. J. Plus* **137** 62
[15] Lu H, Zheng W and Jiang Q 2007 *J. Phys. D: Appl. Phys.* **40** 320
[16] Evans R F L, Atxitia U and Chantrell R W 2015 *Phys. Rev. B* **91** 144425
[17] Diop L, Kuz'min M, Skokov K, Karpenkov D Y and Gutfleisch O 2016 *Phys. Rev. B* **94** 144413
[18] Crangle J and Goodman 1971 *Proc. Roy. Soc. Lond. A Math. Phys. Sci.* **321** 477
[19] Bloch F 1930 *Zeitschrift. für Physik.* **61** 206
[20] Bastardis R, Atxitia U, Chubykalo-Fesenko O and Kachkachi H 2012 *Phys. Rev. B* **86** 094415
[21] Chikazumi S and Graham C D 1997 *Physics of ferromagnetism* (Vol. 94) (London: Oxford University Press)
[22] Kuz'min 2005 *Phys. Rev. Lett.* **94** 107204
[23] Callen E and Callen H 1965 *J. Appl. Phys.* **36** 1140
[24] Zhang X, Liu L and Liu W 2013 *Sci. Rep-Uk.* **3** 2908
[25] Jiang Z, Li R, Zhang S and Liu W 2005 *Phys. Rev. B* **72** 045201
[26] Chen Y, Tao H, Yao D and Liu W 2012 *Phys. Rev. Lett.* **108** 246402
[27] Li W, Yang F and Fang D 2010 *Acta Mech. Sinica-Pcr.* **26** 235
[28] Li W, Zhang X, Kou H, Wang R and Fang D 2016 *Int. J. Mech. Sci.* **105** 273
[29] He Y, Li W, Yang M, Li Y and Zhang X 2022 *J. Constr. Steel. Res.* **191** 107184
[30] He Y, Li W, Yang M, Zhao Z, Zhang X and Dong P 2022 *Int. J. Fatigue.* **161** 106896
[31] Geng P, Li W, Zhang X, Deng Y, Kou H and Ma J 2017 *J. Alloys Compd.* **706** 340
[32] Zhang X, Li W, Deng Y, Shao J, Kou H and Ma J 2018 *J. Phys. D: Appl. Phys.* **51** 075308
[33] Zhang X, Li W, Kou H, Shao J, Deng Y and Zhang X 2019 *J. Appl. Phys.* **125** 18
[34] Zhang X, Li W, Ma J, Li Y and Zhang X 2021 *J. Alloys Compd.* **851** 156747
[35] Dong P, Zhang X, Ma Y, He Y, Yang J and Li W 2023 *Met. Mater. Int.* **30** 1041
[36] Geng P, Li W, Zhang X, Zhang X, Deng Y and Kou H 2017 *J. Phys. D: Appl. Phys.* **50** 40
[37] Geng P, Li W, Zhang X, Deng Y, Kou H and Chen L 2018 *J. Appl. Phys.* **124** 035703
[38] Zhang X, Li W, Deng Y, Shao J, Geng P and Zhang X 2018 *Mater. Res. Express* **6** 015904
[39] Mørup S, Hansen MF and Frandsen C 2010 *Beilstein. J. Nanotech.* **1** 182
[40] Buschow K H J 1977 *Rep. Prog. Phys.* **40** 1179
[41] Stier M, Neumann A, Philippi-Kobs A, Oepen H P and Thorwart M 2018 *J. Magn. Magn. Mater.* **447** 100
[42] Durst K D and Kronmüller H 1986 *J. Magn. Magn. Mater.* **59** 86
[43] Xiao Y, Morvan F, He A, Wang M and Luo H 2020 *Jiao R. Appl. Phys. Lett.* **117** 13
[44] Konar B 2012 *Critical evaluation and thermodynamic optimization of the iron-rare-earth systems* (Canada: McGill University)
[45] Mandal K, Yan A, Kerschl P, Handstein A, Gutfleisch O and Müller K J 2004 *J. Phys. D: Appl. Phys.* **37** 2628
[46] Gray D E and Henry W 1957 *Phys. Today* **10** 36
[47] Pauthenet R 1982 *J. Appl. Phys.* **53** 8187
[48] Weiss P and Forrer R 1925 *Ann. Physique.* **10** 153
[49] Kuz'min M, Chernyshov A, Pecharsky V, Gschneidner Jr K and Tishin A 2006 *Phys. Rev. B* **73** 132403
[50] Amitin E, Bessergenev W, Kovalevskaya Y A and Paukov I 1983 *J. Chem. Thermodynamics* **15** 181
[51] Jennings L, Stanton R and Spedding F 1957 *J. Chem. Phys.* **27** 909
[52] Koyama K, Fujii H and Canfield P C 1996 *Physica B* **226** 363
[53] Hanindriyo A T 2021 *Ab initio assessment of computational thermodynamics applied to magnetic alloys* (Japan: Japan Advanced Institute of Science and Technology)
[54] Buschow K H J and Boer F R 2003 *Physics of magnetism and magnetic materials* (Vol. 7) (New York: Kluwer Academic/Plenum Publishers)
[55] Callen H B and Callen E 1966 *J. Phys. Chem. Solids.* **27** 1271
[56] Van vleck J H 1937 *Phys. Rev.* **52** 1178
[57] Zener C 1954 *Phys. Rev.* **96** 1335